

A Modeling Study of the Influence of Ice Scavenging on the Chemical Composition of Liquid-Phase Precipitation of a Cumulonimbus Cloud

NICOLE AUDIFFREN, SYLVIE CAUTENET, AND NADINE CHAUMERLIAC

LAMP, Laboratoire de Météorologie Physique, CNRS, and Université Blaise Pascal, Aubiere, France

(Manuscript received 7 April 1997, in final form 27 September 1998)

ABSTRACT

Evidence of the efficient removal of chemicals by ice particles has been deduced from past field experiments and laboratory studies. However, the ice phase has been poorly represented in prior cloud chemistry modeling. This paper uses a two-dimensional Eulerian cloud model to address the impact of ice-phase processes on the chemistry of precipitation in the context of a simulated cumulonimbus cloud. Riming of graupel and the freezing of supercooled rain are the main processes for the transfer of species toward graupel. Even when freezing is the main mode for this transfer, riming still plays an important role by providing a feedback effect that limits the diluting influence of rain. When riming is the only process, sulfate production is more efficient in rainwater, whereas when freezing dominates a decrease in sulfate production is observed.

During the decaying stage, the precipitation (glaciated and/or liquid) has higher concentrations of the hydrogen peroxide and sulfates that originated from the gas phase. However, sulfates chemically produced in the liquid phases are less concentrated than if ice had played no role.

This study demonstrates the potential impact of ice-phase processes in organized cloud systems where strong updrafts exist, as ahead of a cold front.

1. Introduction

Clouds can be thought of as an efficient engine processing atmospheric air and its trace constituents. Their dynamical effects play an important role in the redistribution of heat, vapor, and trace constituents of the air. They also act as a chemical aqueous-phase reactor, and they filter certain portions of atmospheric trace components from the air, depositing them on the ground in liquid or solid forms of precipitation. Hence, clouds have the general effect of cleaning the atmosphere, though they thereby also induce acidic precipitation. Chemicals that are not deposited within storms can be injected into the upper troposphere, after which they contribute to the background atmosphere. Strong convective cells are able to penetrate the mean tropopause level and bring products to the lower stratosphere.

For several years, particular attention has been paid to acidic rain (Chameides 1984; Daum et al. 1984; Kelly et al. 1985; Tremblay and Leighton 1986; Chaumerliac et al. 1991; and others). The primary tool used in these earlier studies has been regional-scale models in which

chemicals were fractionated according to microphysical processes governing liquid-phase exchanges.

Nevertheless, precipitation is often initiated in mixed-phase parts of the clouds where additional effects of species partitioning can occur. The role of ice-phase processes has been studied in the past first from a dynamical point of view. Inclusion of ice microphysics in cloud modules gives a better description of cloud and precipitation formation processes. Latent heat released during growth by vapor deposition, riming, and the freezing of rain strongly enhances the cloud growth, affects the formation of the precipitation, and of course alters the structure of circulation fields (Orville and Kopp 1977; Zhang 1989; Cotton et al. 1982). The consideration of ice nucleation in the dynamics can significantly change the results for the deposition rates and the concentrations of chemical species in a spectral microphysical model (Respondek et al. 1995). Mölder et al. (1994) pointed out several main differences in the chemical behavior when ignoring cold-cloud processes in convective or stratiform clouds. According to them, including ice-phase processes in dynamics modeling leads to lower values of sulfate in the liquid phase when convection is present. Available liquid water content is reduced when ice-phase processes are taken into account. The effect of this reduction can be seen from gas-phase concentrations of sulfur dioxide showing reduced values. In convective clouds, competition exists between aqueous-phase chemical production and dilution by en-

Corresponding author address: Dr. Nicole Audiffren, Laboratoire de Météorologie Physique, CNRS, and Université Blaise Pascal, 24 Av. des Landais, 61377 Aubiere Cedex, France.
E-mail: audiffre@opgc.univ-bpclermont.fr

trainment and/or washout. The balance of these two last processes will determine the possible enhancement of sulfates and hydrogen peroxide in the gaseous phase. One can expect that the result of this balance may differ from one cloud involving ice to another. Moreover, if ice-phase processes are taken into account in the exchanges of species between different classes of hydrometeors, previous results could be strongly modified with changes in scavenging rates, as experimentally observed by Topol (1986). The fraction of species retained in ice would not participate in the aqueous-phase chemistry but rather would be released into atmospheric layers that are undersaturated relative to ice. Such detrainment events would alter the chemical composition of the low layers even though the ice-phase processes took place in upper levels.

Direct freezing of droplets and their hydrodynamical collection by sedimenting ice particles constitute alternative ways for the removal of species, disturbing the usual interphase transfer. During field experiments Murakami et al. (1983) observed that below-cloud sulfate particles were removed by snow twice as efficiently as by rain.

Direct uptake of aerosol particles by snow or hail seems to be particularly efficient. Laboratory studies (Mittra et al. 1990) show that substantial amounts of SO_2 can be adsorbed onto ice surface during growth of snow crystals by vapor deposition, while the entrapped fraction of SO_2 becomes negligible once the crystals have ceased their growth. However, Diehl et al. (1996) have emphasized that the uptake of gaseous chemicals by snow via adsorption is less rapid than the uptake by drops. Much larger quantities are thus accommodated by a drop than by an ice crystal of the same water mass. Hence, it is expected that in the lower troposphere the microphysical processes linked to the ice-phase and relevant for the scavenging of chemicals are those involving exchanges with the liquid phase rather than with the gas phase directly. Among them, riming and the freezing of drops are likely to be the dominant processes. Their relative importance will depend on the stage of development of the cloud. Riming covers the highest spatial extent in the cloud compared to interactions between rain and graupel.

Direct uptake of chemical species (adsorption) by ice becomes important when larger exposure times of snow particles are involved, as is the case for fresh ground-deposited snow. Until the next snowfall event adsorption/desorption of the chemical species will probably affect the composition of the snow at the surface (Sigg et al. 1992). The knowledge of this process (as well as possible diffusion into the ice lattice) is important for chemical retrieval of past atmospheres from ice core analyses. Nevertheless, to assess the relative contribution of this process compared to the others, one needs to know the exchange of species in the cold-precipitating cloud that yielded the snowfall.

Two-dimensional kinetic models including ice phase

chemistry have been formulated by Hegg et al. (1984, 1986), Barth et al. (1992), Leighton et al. (1990), and Rutledge et al. (1986) to study scavenging in warm- and cold-frontal rainbands. Whereas Leighton et al. (1990) found no impact of ice on rain sulfate concentrations because the 0°C isotherm was well above the scale height of the sulfur dioxide profile, Barth et al. (1992) showed significant amounts of sulfate and hydrogen peroxide to exist in ice particles of cold-frontal rainbands. Hence, the impact of ice-phase chemistry has not clearly been assessed, particularly for gas-phase concentrations.

Besides the evaluation of the amount of acid precipitation in regional models in order to drive some parameterizations (e.g., Song and Leighton 1996) for global chemistry models, it is of interest to assess the extent to which an isolated cloud alters gas-phase concentrations and how long these remain disturbed after the cloud event. This last point is particularly relevant for organized cloud systems, in which clouds succeed rapidly one after another. Strong convective clouds are very efficient at transporting ground-emitted chemical products to higher altitudes where mixed-phase conditions exist. These conditions can be found at the rear of the warm sector just ahead of the cold front where significant updrafts advect substantial amounts of pollutants to ice levels through a zone of liquid water. From a chemical point of view, it is important to discriminate the processes involving the ice-phase during the cloud lifetime in order to spare computational costs for irrelevant processes and to help find suitable parameterizations for larger-scale models.

In this paper, we investigate the role of ice-phase processes on the chemistry in the case of an isolated strong convective cloud system. Exchanges of species with the ice particles will be limited to interactions with cloud water and rainwater. This study employs a two-dimensional model and aims to evaluate the relative importance of various microphysical processes on the cloud chemistry using the latest laboratory findings relative to uptake of chemical species by ice.

2. Description of the model

The cloud model is a two-dimensional (x, z) time-dependent Eulerian scheme (Cautenet and Lefevre 1994). It is nonhydrostatic and anelastic. Both horizontal and vertical grid resolutions are of 200 m and the overall dimension of the domain is $11 \text{ km} \times 11 \text{ km}$. The microphysical code uses four classes of hydrometeors: cloud water, rain, cloud ice and snow, and graupel (or hail). The scheme of Kessler (1969) is used for the cloud droplet coalescence with a threshold put at 1 g kg^{-1} and rain distribution follows the scheme of Marshall and Palmer (1948). Cloud ice and snow are regrouped into the same category. The reader is referred to these publications for further details. Hereafter, some features that are most relevant for chemistry are summarized. The cloud droplet population is monodisperse

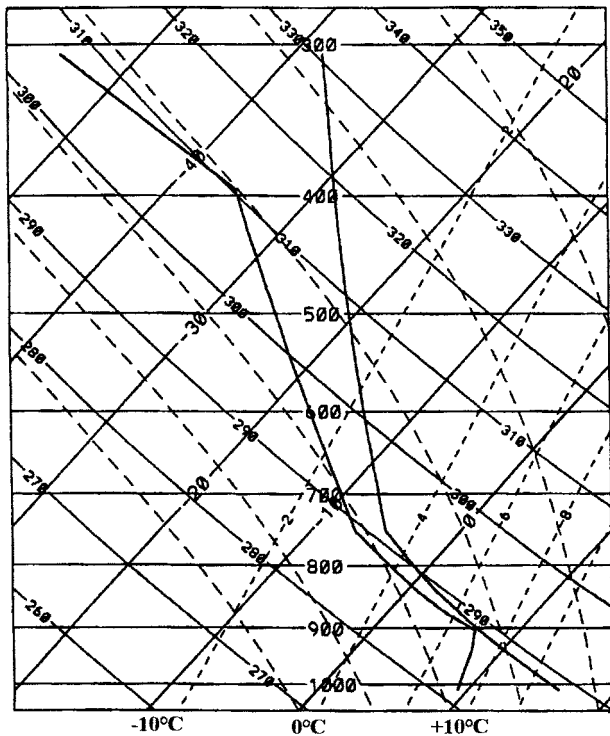


FIG. 1. Temperature and dewpoint profiles from Reisin et al. (1996).

and time invariant (the total number of droplets is fixed). Precipitation and graupel distributions are described by a Marshall and Palmer (1948) distribution. The precipitation distribution is fixed by the intercept, while the graupel distribution is determined using a fixed total number concentration of graupel particles. This number concentration has been chosen according to observations made by Cotton et al. (1982) and is 100 m^{-3} . The total number of ice particles is calculated using a form of Fletcher's relation as modified by Taylor (1989a,b) to permit snow concentrations greater than 0.01 g kg^{-1} to exist in regions with temperatures above -12°C , which are favorable for rapid snow-to-graupel conversion. Homogeneous nucleation occurs when the total number of ice particles exceeds 10^7 , that is, around -37°C . Finally, terminal speeds of glaciated hydrometeors are calculated according to the parameterization used by Wang and Chang (1993) thus providing more realistic values than those issued from the formulation used by Taylor (1989a).

3. Cloud features

The vertical profiles of temperature and dew point are those used in the study of Reisin et al. (1996) and are shown in Fig. 1. The 0°C isotherm is located at 1900 m. For initialization a pulse of heat that produced a 2°C perturbation was applied for one time step, at $t = 0$, between 200 and 2400 m on each 400 m of the axis.

The cloud base and top are, respectively, at the altitudes of 2000 and 4500 m where the temperature is -19°C .

During the growth phase (Fig. 2), which lasts for the first 14 min, few cloud ice particles are produced, while freezing of large drops efficiently contributes to a source of graupel. Snow-to-graupel conversion, favored by using the formulation of Taylor (1989a), induces a rapid disappearance of cloud ice (maximum content lower than 0.1 g kg^{-1} after 12 min). Riming essentially concerns graupel that comes from freezing of large drops. These latter appear earlier because of a low threshold of autoconversion of cloud droplets into rain. As found by Reisin et al. (1996), riming plays an important role in the formation of graupel. Although we chose the same profiles as these authors, the cloud model differs from theirs and so some differences are observed. The number concentration of cloud droplets and graupel particles are fixed in our model. The general features are retrieved with a maximum updraft of 20 m s^{-1} , a maximum liquid water content (LWC) of 3.5 g kg^{-1} , 0.3 g kg^{-1} , and 1.7 g kg^{-1} , respectively, for the maxima of cloud, ice, and graupel. These features are close to the "moderate continental case" of Reisin et al. (1996), although rain starts earlier in our model.

Between 15 and 25 min (Fig. 3) is the mature stage of the cloud with quite constant maxima of the LWC and graupel. At 24 min (Fig. 3) rain and graupel have reached the ground. The beginning of the decaying stage (Fig. 4) is at 30 min where a net decrease in the LWC is observed. Consequently, the riming process of graupel is slowing down.

4. Chemical module

Aqueous and gas phase chemistries related to the methane oxidation chain and sulfur dioxide are treated. Sulfate and ammonium aerosol scavenging are included in the model. Vertical profiles are chosen constant (in ppb) with height and are typical of mean values observed in remote areas (continental). The mass concentrations of ammonium and sulfate aerosols are initialized, respectively, to $0.08 \mu\text{g m}^{-3}$ and $5 \mu\text{g m}^{-3}$. Tables 1–4 list the reactions and initial chemical concentrations. Values are typical of a moderately polluted continental area with NO_x put at 18 ppt, 140 ppb for CO , 25 ppb for ozone, 2 ppb for H_2O_2 , and 1 ppb for SO_2 . Moderately polluted conditions essentially apply to H_2O_2 and SO_2 . The NO_x , CO , O_3 values are typical of remote areas. The initial levels for the soluble species H_2O_2 and SO_2 have deliberately been put at quite high values since there will be no fluxes at the ground during the simulations.

A first set of runs has been conducted without sulfate aerosols, with the aim of focusing on possible modifications of sulfate productions. Another set of runs with sulfate aerosols will give some information on the capability of ice at capturing them.

Oberholzer et al. (1993) reported pollutant concen-

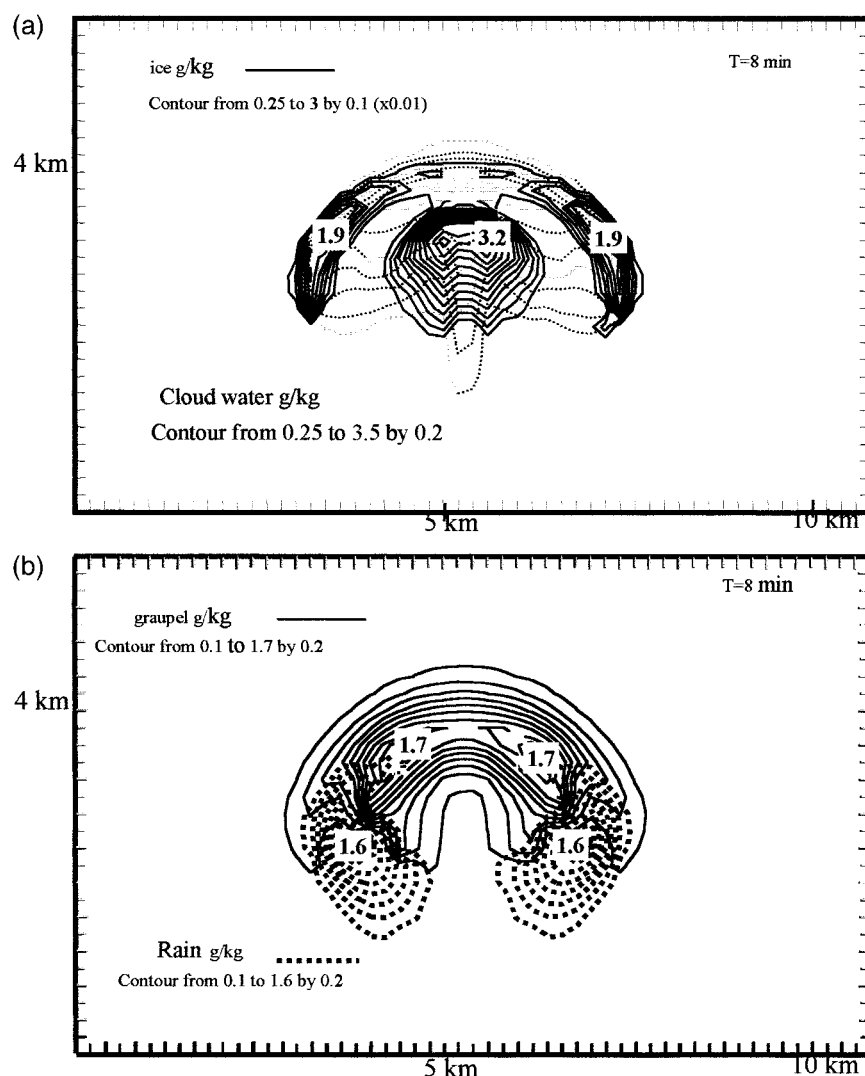


FIG. 2. Cloud during the development stage $t = 8$ min.

trations in winter cloud water and precipitation. They found that when the molar concentration ratio of gaseous ammonia and ammonium aerosol was low (below 1/1), the pH was constant from the bottom of the cloud (ratio 1/1) to the middle of the cloud (ratio 1/9) at a value just above 4. They also found that pH can reach values above 5 and evolves from the bottom of the cloud to the middle parts of it when the concentration ratio exceeds the value of 2. Here, there is no ammonia gas, therefore we chose the pH at the value of 4.16. At this value of pH, only the oxidation by hydrogen peroxide is to be considered.

5. Ice-phase chemistry

Entrapment of chemical products during riming ice (snow or graupel) has been parameterized using recent laboratory results. We adopt the formulation of Lamb

and Blumenstein (1987) for the entrapped fraction of a product into ice crystal

$$f = 0.012 + 0.0058(T_0 - T),$$

where T is the drop temperature (taken as the ambient temperature) before cooling. Even though this parameterization has been established for S(IV), we adopt it for all the species except SO_2 and hydrogen peroxide. According to Snider et al. (1992) a value of 0.3 is taken for the retention coefficient for H_2O_2 . The formulation of Lamb and Blumenstein (1987) is applied for the range of ambient temperatures encountered over the whole simulated cloud (Fig. 5) and gives a value between 3×10^{-2} and 0.12.

For SO_2 , the uptake during riming is parameterized according to Iribarne and Barrie (1995), who investigated the oxidation of S(IV) during the riming of cloud droplets. From their results we extract a formulation of

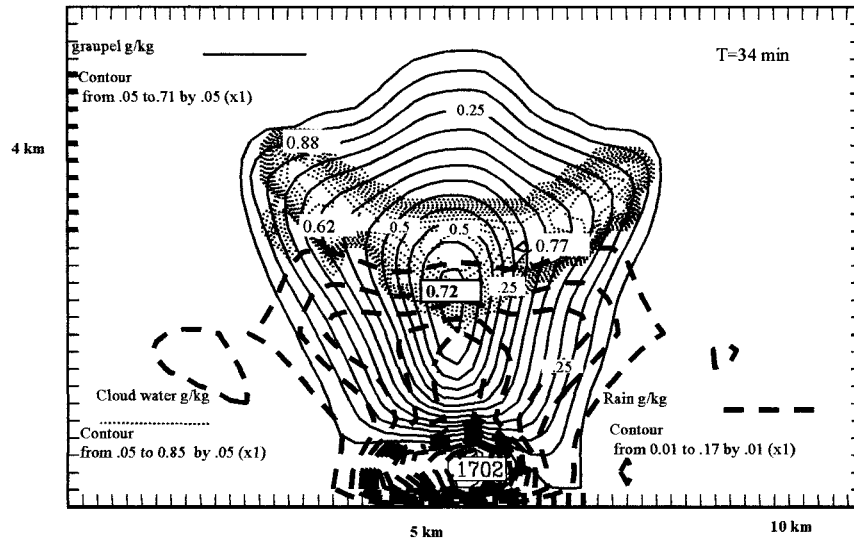


FIG. 3. Cloud during its mature stage $t = 24$ min.

the fraction of S(IV) in the riming droplet oxidized to sulfate and the fraction retained by ice as S(IV) as a function of the ratio $NH_4^+/S(IV)$. Two regimes are distinguished: dry growth between -9° and $-12^\circ C$ and wet growth riming between -3° and $-6^\circ C$. In both of these regimes the coefficients are linearly dependent on the ratio $NH_4^+/S(IV)$. Between -3° and $-9^\circ C$, the retention coefficient has been chosen as a linear interpolation of its bounding values in the two other regimes. It is found that over the entire cloud and for all the duration of the simulation it is found that the retention coefficient of SO_2 keeps a value around 0.4.

No adsorption of gases is simulated because this process is still poorly understood for the species we are concerned with (H_2O_2 , SO_2). We therefore focus on the

exchange of such trace gases between the liquid phase and ice phase and their consequences on rain chemical contents and gas-phase concentrations.

6. Chemical results

We first discuss results when aerosols are not present initially. A first run (referred as ice run in the following) takes into account the presence of ice in the chemical module while a second run (referred to as no-ice run) considers effects of the redistribution of species by microphysical processes concerning only the liquid phase. Chemical reactions in the gas and aqueous phases are kept on in both runs.

The impact of the ice phase on the scavenging of

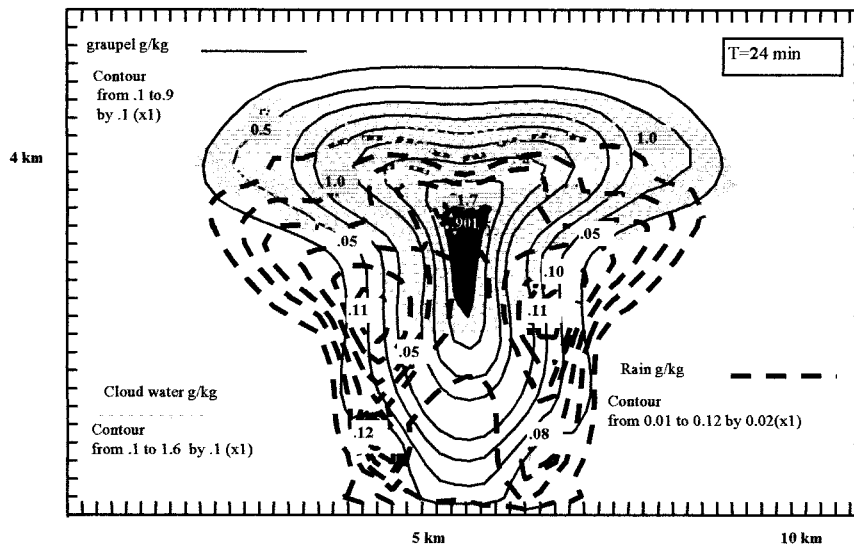


FIG. 4. Cloud during its decaying stage $t = 34$ min.

TABLE 1. List of the reactions and equilibrium in the gas phase with corresponding rate and equilibrium constants [from Lelieveld and Crutzen (1991), G27 from De More et al. (1994), G4 modified by Stockwell (1994)].

Gas-phase reaction scheme		Rate constants
G1 ^c	$O_3 + H_2O + h\nu \rightarrow 2OH^\cdot + O_2$	J_{eff}
G2	$O_3 + OH^\cdot \rightarrow HO_2 + O_2$	$1.6 \times 10^{-12} \exp(-940/T)$
G3	$O_3 + HO_2 \rightarrow OH^\cdot + 2O_2$	$1.1 \times 10^{-14} \exp(-500/T)$
G4	$2HO_2 \rightarrow H_2O_2 + O_2$	$[2.3 \times 10^{-13} \exp(600/T) + 1.7 \times 10^{-33} [M] \exp(1000/T)] \times [1 + 1.4 \times 10^{-21} [H_2O] \exp(2200/T)]$
G5	$H_2O_2 + h\nu \rightarrow 2OH^\cdot$	4.6×10^{-6}
G6	$H_2O_2 + OH^\cdot \rightarrow HO_2 + H_2O$	$3.3 \times 10^{-12} \exp(-200/T)$
G7	$CH_4 + OH^\cdot + O_2 + M \rightarrow CH_3O_2 + H_2O + M$	$2.3 \times 10^{-12} \exp(-1700/T)$
G8	$CH_3O_2 + HO_2 \rightarrow CH_3O_2H + O_2$	4.0×10^{-12}
G9	$CH_3O_2H + O_2 + h\nu \rightarrow CH_2O + HO_2 + OH^\cdot$	4.6×10^{-6}
G10	$CH_3O_2H + OH \rightarrow CH_3O_2 + H_2O$	5.6×10^{-12}
G11	$CH_3O_2H + OH \rightarrow CH_2O + OH^\cdot + H_2O$	4.4×10^{-12}
G12	$CH_2O + 2O_2 + h\nu \rightarrow CO + 2HO_2$	1.7×10^{-5}
G13	$CH_2O + h\nu \rightarrow CO + H_2$	3.3×10^{-5}
G14	$CH_2O + OH^\cdot + O_2 \rightarrow CO + HO_2 + H_2O$	1.1×10^{-11}
G15	$CO + OH^\cdot + O_2 + M \rightarrow CO_2 + HO_2 + M$	2.4×10^{-13}
G16	$NO + O_3 \rightarrow NO_2 + O_2$	$2.0 \times 10^{-12} \exp(-1400/T)$
G17	$NO_2 + O_2 + h\nu \rightarrow NO + O_3$	5.6×10^{-3}
G18	$NO + HO_2 \rightarrow NO_2 + OH^\cdot$	$3.7 \times 10^{-12} \exp(240/T)$
G19	$NO + CH_3O_2 + O_2 \rightarrow NO_2 + CH_2O + HO_2$	$4.2 \times 10^{-12} \exp(180/T)$
G20	$NO_2 + OH (+ M) \rightarrow HNO_3 (+ M)$	1.2×10^{-11}
G21	$HNO_3 + h\nu \rightarrow NO_2 + OH$	3.2×10^{-7}
E22	$CH_2O + HO_2 \leftrightarrow O_2CH_2OH$	6.7×10^{-15}
G23	$O_2CH_2OH + HO_2 \rightarrow HCO_2H + HO_2 + O_2$	2.0×10^{-12}
G24	$O_2CH_2OH + NO + O_2 \rightarrow HCO_2H + HO_2 + NO_2$	7.0×10^{-12}
G25	$O_2CH_2OH + O_2CH_2OH \rightarrow 2HCO_2H + HO_2 + H_2O$	1.2×10^{-13}
G26	$HCO_2H + OH + O_2 \rightarrow CO_2 + HO_2 + H_2O$	3.2×10^{-13}
G27	$SO_2 + OH (+ M) \rightarrow H_2SO_4 + HO_2$	$k_\infty = 1.5 \times 10^{-12}; Fc = 0.6; k_0 = 3. \times 10^{-31}(T/300)^{-3.3}$

* Reaction rate constants of first-order reactions are in s^{-1} , of second-order reactions in molecule⁻¹ cm³ s⁻¹.

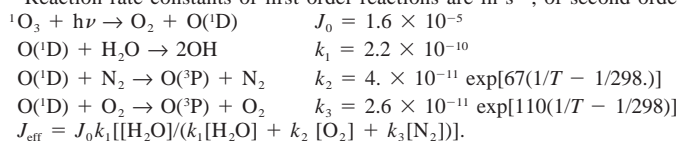


TABLE 2. List of the gas-aqueous phase equilibria with corresponding Henry's law constants and of aqueous equilibria with corresponding dissociation constants (from Lelieveld and Crutzen 1991).

Gas-aqueous and aqueous phase equilibria		Henry's law and dissociation constants K_{298}^\ddagger
E1	$H_2O \leftrightarrow H^+ + OH^-$	$1.0 \times 10^{-14} \exp[-6716(1/T - 1/298)]$
H1	$O_3 (\text{gas}) \leftrightarrow O_3 (\text{aq})$	$1.1 \times 10^{-2} \exp[2300(1/T - 1/298)]$
H2	$H_2O_2 (\text{gas}) \leftrightarrow H_2O_2 (\text{aq})$	$7.4 \times 10^4 \exp[6615(1/T - 1/298)]$
E2	$H_2O_2 (\text{aq}) \leftrightarrow HO_2^- + H^+$	$2.2 \times 10^{-12} \exp[-3730(1/T - 1/298)]$
H3	$CH_3O_2H (\text{gas}) \leftrightarrow CH_3O_2H (\text{aq})$	$2.2 \times 10^2 \exp[5653(1/T - 1/298)]$
H4	$CH_2O (\text{gas}) \leftrightarrow CH_2(OH)_2 (\text{aq})$	$6.3 \times 10^3 \exp[6425(1/T - 1/298)]$
H5	$HNO_3 (\text{gas}) \leftrightarrow HNO_3 (\text{aq})$	$2.1 \times 10^5 \exp[8700(1/T - 1/298)]$
E3	$HNO_3 (\text{aq}) \leftrightarrow H^+ + NO_3^-$	15.4
H6	$HO_2 (\text{gas}) \leftrightarrow HO_2 (\text{aq})$	$2.0 \times 10^3 \exp[6600(1/T - 1/298)]$
E4	$HO_2 (\text{aq}) \leftrightarrow H^+ + O_2^- (\text{aq})$	3.5×10^{-5}
H7	$OH^\cdot (\text{gas}) \leftrightarrow OH^\cdot (\text{aq})$	$25 \exp[5025(1/T - 1/298)]$
H8	$NO_2 (\text{gas}) \leftrightarrow NO_2 (\text{aq})$	$6.4 \times 10^{-3} \exp[2500(1/T - 1/298)]$
H9	$NO (\text{gas}) \leftrightarrow NO (\text{aq})$	$1.9 \times 10^{-3} \exp[1480(1/T - 1/298)]$
H10	$CH_3O_2 (\text{gas}) \leftrightarrow CH_3O_2 (\text{aq})$	$2.0 \times 10^3 \exp[6600(1/T - 1/298)]$
H11	$HCO_2H (\text{gas}) \leftrightarrow HCO_2H (\text{aq})$	$3.7 \times 10^3 \exp[5700(1/T - 1/298)]$
E5	$HCO_2H (\text{aq}) \leftrightarrow H^+ + HCO_2^-$	$1.8 \times 10^{-4} \exp[-1510(1/T - 1/298)]$
H12	$SO_2 (\text{gas}) \leftrightarrow SO_2 (\text{aq})$	$1.2 \exp[3120(1/T - 1/298)]$
E6	$SO_2 (\text{aq}) \leftrightarrow H^+ + HSO_3^-$	$1.7 \times 10^{-2} \exp[-2090(1/T - 1/298)]$
E7	$HSO_3^- \leftrightarrow H^+ + SO_3^{2-}$	$6. \times 10^{-8} \exp[-1120(1/T - 1/298)]$

* Henry's law constants in mol L⁻¹ atm⁻¹ and dissociation constants in mol L⁻¹ at 298 K.

TABLE 3. List of the reactions in the aqueous phase with corresponding rate constants (from Lelieveld and Crutzen 1991).

	Aqueous phase reaction scheme	Rate constants at 298 K*
A1	$\text{H}_2\text{O}_2 + h\nu \rightarrow 2\text{OH}\cdot$	$G5 \times 1.6$ (in s^{-1})
A2	$\text{O}_3 + h\nu \rightarrow \text{H}_2\text{O}_2 + \text{O}_2$	$G1 \times 1.6$ (in s^{-1})
A3	$\text{CH}_2(\text{OH})_2 + \text{OH}\cdot + \text{O}_2 \rightarrow \text{HCO}_2\text{H} + \text{HO}_2 + \text{H}_2\text{O}$	$2.0 \times 10^9 \exp[-1500(1/T - 1/298)]$
A4	$\text{HCO}_2\text{H} + \text{OH}\cdot + \text{O}_2 \rightarrow \text{CO}_2 + \text{HO}_2 + \text{H}_2\text{O}$	$1.6 \times 10^8 \exp[-1500(1/T - 1/298)]$
A5	$\text{HCO}_2^- + \text{OH}\cdot + \text{O}_2 \rightarrow \text{CO}_2 + \text{HO}_2 + \text{OH}^-$	$2.5 \times 10^9 \exp[-1500(1/T - 1/298)]$
A6	$\text{O}_3 + \text{O}_2 \xrightarrow{\text{H}_2\text{O}} \text{OH}\cdot + \text{OH}^- + 2\text{O}_2$	$1.5 \times 10^9 \exp[-1500(1/T - 1/298)]$
A7	$\text{HO}_2 + \text{O}_2^- + \text{H}_2\text{O} \rightarrow \text{H}_2\text{O}_2 + \text{OH}^- + \text{O}_2$	$1.0 \times 10^8 \exp[-1500(1/T - 1/298)]$
A8	$\text{H}_2\text{O}_2 + \text{OH}\cdot \rightarrow \text{HO}_2 + \text{H}_2\text{O}$	$2.7 \times 10^7 \exp[-1715(1/T - 1/298)]$
A9	$\text{CH}_3\text{O}_2 + \text{O}_2^- + \text{H}_2\text{O} \rightarrow \text{CH}_3\text{O}_2\text{H} + \text{OH}^- + \text{O}_2$	$5.0 \times 10^7 \exp[-1610(1/T - 1/298)]$
A10	$\text{CH}_3\text{O}_2\text{H} + \text{OH}\cdot \rightarrow \text{CH}_3\text{O}_2 + \text{H}_2\text{O}$	$2.7 \times 10^7 \exp[-1715(1/T - 1/298)]$
A11	$\text{SO}_3^{2-} + \text{O}_3 \rightarrow \text{SO}_4^{2-} + \text{O}_2$	$1.9 \times 10^7 \exp(-1860(1/T - 1/298))$
A12	$\text{SO}_3^{2-} + \text{OH} \rightarrow \text{SO}_4^{2-} + \text{OH}^-$	$5.5 \times 10^9 \exp[-1500(1/T - 1/298)]$
A13	$\text{HSO}_3^- + \text{OH} + \text{O}_2 \rightarrow \text{SO}_3^- + \text{H}_2\text{O}$	$9.5 \times 10^9 \exp[-1500(1/T - 1/298)]$
A14	$\text{HSO}_3^- + \text{H}_2\text{O}_2 \rightarrow \text{SO}_4^{2-} + \text{H}_2\text{O} + \text{H}^+$	$7.45 \times 10^7 \exp[-4725(1/T - 1/298)]$

* Rate constants are in $\text{mol L}^{-1} \text{s}^{-1}$ (except for A1 and A2).

chemical species can be analyzed following two different approaches. One considers the concentrations of the species over the entire phase (gas, cloud water, or rainwater). Another approach is based on the calculation, at each grid point in the domain and at each time, of the difference between the concentrations given by the two runs. This method illustrates well the locations of the observed maxima, whereas the former gives information on how the budget of the washout is altered by the action of ice on chemistry.

During the *first 14 min*, a large fraction of raindrops are converted to graupel by freezing that is, at this time, the main mode of transfer of hydrogen peroxide to graupel (75% of the quantity of species exchanged with graupel, see Fig. 6). The second mode of transfer for hydrogen peroxide is thus riming. However, for S(IV), although the prevailing mode of transfer to ice is also freezing of raindrops, riming does play a significant role (Fig. 7) while it is negligible for hydrogen peroxide. For instance, at 8 min riming still represents only 20% for S(IV) transferred to graupel.

When ice is not accounted for, 20% more (on average) is observed for the total concentration of hydrogen peroxide in the condensed phases (Fig. 8). No differences are visible on the cloud water H_2O_2 content (Fig. 9) as in gas-phase concentrations (Fig. 10).

A loss of the total quantity of S(IV) (Fig. 11) over all condensed phases is also observed when ice plays its role in chemistry. Since a loss over the total quantity happens, there is, therefore, not only a transfer of H_2O_2 and SO_2 to ice through the freezing of raindrops. Moreover, there is an increase in gas-phase sulfate concentration (Fig. 12). Sulfates and S(IV) are lost by riming. The retention coefficient for S(VI) is taken as the same as for SO_2 . This latter is low and S(IV) can return to

cloud water as soon as it has been released during riming. Compared with the case where the ice does not play any role (no-ice run) on the redistribution of species, there is less S(IV) available to be transferred toward rain but more can be oxidized in sulfate. This process is subsequent to the transfer rate of S(IV) by riming and its loss to gas phase. Hence, any sulfate, produced in excess compared to the no-ice run, is readily found in the gas phase (Fig. 12) after being released by riming. When freezing of raindrops and riming exist simultaneously, riming has a feedback effect on the decrease of S(IV) concentration (Fig. 13) in rain by opening a new way for SO_2 to escape from cloud water or being oxidized. Enhanced oxidation in cloud water also leads to reduced H_2O_2 available for transfer toward rain (Fig. 9) and subsequently the total quantity in condensed phases (Fig. 8).

During the following 10 min, riming and freezing play a different role according to the species. The SO_2 and H_2O_2 behaviors are out of phase. For SO_2 , there is still from time to time a competition between freezing and riming (Fig. 7), each of them being alternatively the dominant process for transfer to ice. From 24 min, the impact of riming is visible on the aqueous (cloud water) concentration of H_2O_2 .

From 14 to 18 min, freezing does not play any role. Hence, rain has ceased to lose SO_2 (for the ice run). The differences between the ice run and the no-ice run on the S(IV) concentration in rainwater are reducing. However, there is still less H_2O_2 in rain (Fig. 9) when ice is accounted for, and the difference on this quantity is increasing. That means that the production of sulfate in rainwater is more efficient in the ice run (Figs. 14 and 15).

Between 16 and 18 min the quantity of H_2O_2 in rain

TABLE 4. Initial values of the chemical species.

O_3	H_2O_2	SO_2	$\text{CH}_3\text{O}_2\text{H}$	CH_2O	CO	HNO_3	HO_2	OH	NO_2	NO	CH_3O_2	COOH
25 ppb	2 ppb	1 ppb	2 ppb	0.5 ppb	140 ppb	200 ppt	9 ppt	0.08 ppt	12 ppt	6 ppt	9 ppt	0.3 ppt

TABLE 5. Values of the sticking coefficients.

Species	Sticking coefficient	Reference
O ₃	2 × 10 ⁻³	Utter et al. (1992)
H ₂ O ₂	0.18	Ponche et al. (1993)
CH ₃ O ₂ H	0.05	Worsnop et al. (1992)
CH ₂ O	0.05	Lelieveld and Crutzen (1991)
HNO ₃	0.125	van Doren et al. (1990)
HO ₂	0.2	Lelieveld and Crutzen (1991)
OH	0.05	Lelieveld and Crutzen (1991)
NO ₂	6.3 × 10 ⁻⁴	Lelieveld and Crutzen (1991)
NO	1 × 10 ⁻⁴	Lelieveld and Crutzen (1991)
CH ₃ O ₂	0.05	Lelieveld and Crutzen (1991)
HCOOH	0.05	Lelieveld and Crutzen (1991)

decreases while SO₂ remains as it was before. The H₂O₂ rainwater concentration (Fig. 9) drops because riming efficiently takes up H₂O₂ in cloud water. The direct effect of riming works, therefore, first to the detriment of the transfer from cloud water to rainwater before it can be seen on concentrations in cloud water, which is the case after 24 min. Riming increases the differences in the gas phase. Higher concentrations are obtained if ice has played its role on chemistry (Fig. 10).

From 20 to 25 min, H₂O₂ keeps on the same behavior as before whereas SO₂ tendency is again governed by the freezing process. Freezing leads again to S(IV) in rain (20% less than the no-ice run), thus reducing the sulfate production in rain and less sulfate content in condensed phases. The quantity of sulfate in gas phase is then constant, remaining 100 times higher than in the no-ice run.

From 26 min, freezing has completely ceased. The

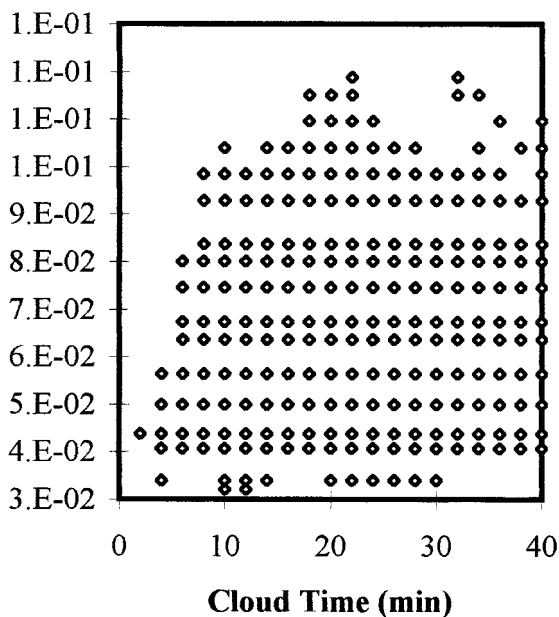


FIG. 5. Retention coefficient for all species except SO₂ and H₂O₂, calculated with the formulation of Lamb and Blumenstein (1987).

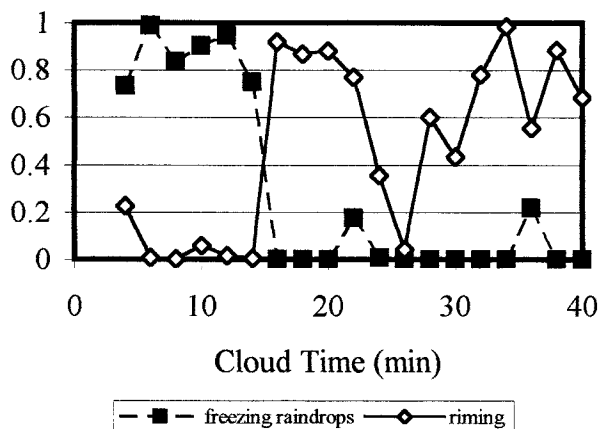


FIG. 6. Relative contribution of riming and freezing in the budget of H₂O₂ exchanged by graupel. A budget of hydrogen peroxide exchanged by graupel is done each 2 min for a 2-min period all over the cloud. Another budget over this period is done for the quantity given to graupel by riming (freezing). The ratio of these budgets is shown on this figure.

cloud has reached its mature stage and sedimentation effects compete with riming on the budget of species exchanged by graupel with cloud and rain waters. The cessation of freezing has, in a first time (until 30 min), the following effect on SO₂ and H₂O₂: loss of their content in rain by freezing ceases and there is a refeeding of rain through cloud water whose concentration is enhanced by a fraction of the quantity lost in gas phase during riming. The differences between the two runs are diminishing for S(IV). The H₂O₂ rainwater and cloud

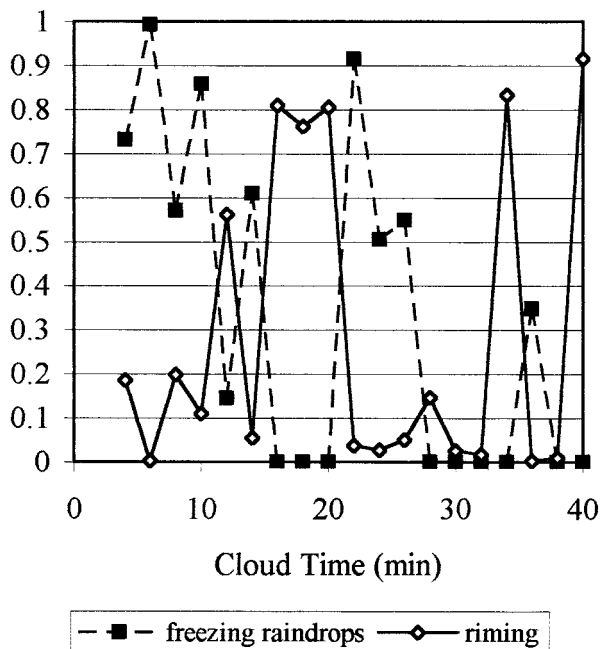


FIG. 7. Same as for Fig. 6 but for SO₂.

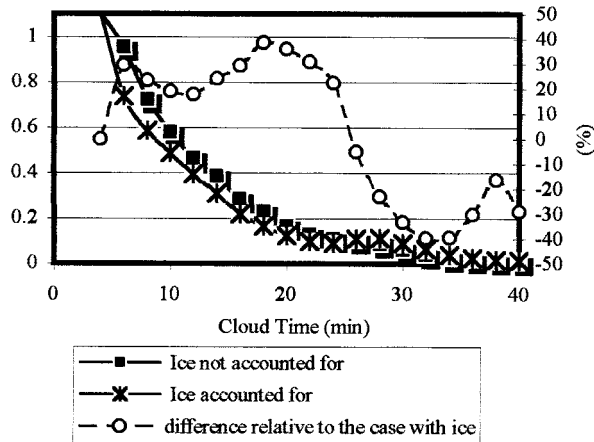


FIG. 8. Mean concentration of H_2O_2 in condensed phases, in ppbv air, averaged over the entire cloud.

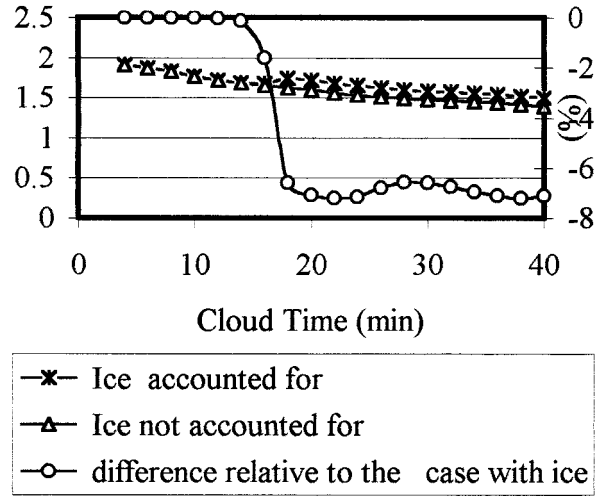


FIG. 10. Mean gas-phase hydrogen peroxide concentration in ppbv air (averaged over the entire domain $11 \text{ km} \times 11 \text{ km}$).

water concentrations are now higher for the ice run and will remain as it is until the end of the simulation.

After 30 min, the differences in S(IV) increase again between the two runs in rainwater and over all condensed phases. Ten minutes later (end of the run), there is up to 60% less S(IV) in rain when ice was accounted for. Hence, S(IV) appears to be more sensitive than H_2O_2 to the sedimentation effects, which counteract the riming effect. Consequently, sulfate content in condensed phases is decreasing (Fig. 15).

Figure 16 shows how the differences, relative to the ice run (run 1), between the ice and the no-ice (run 2) runs for H_2O_2 at 24 min are distributed. At an altitude of 4 km riming dominates and few differences are found

on the gas-phase concentrations, while below this level and particularly around 2 km the difference can reach 80% more as a result of the accumulation of several effects due to strong mixing by vortices inside the cloud.

Scavenging of sulfates aerosols by graupel

A second set of runs similar to the first one has been driven with initial aerosols of moderate concentration ($0.5 \mu\text{g m}^{-3}$). Figures 17 and 18 show the differences in sulfate content in rainwater and in all condensed phases between runs with and without aerosols (first set). It can be seen from Fig. 14 that 30% of aerosols, scav-

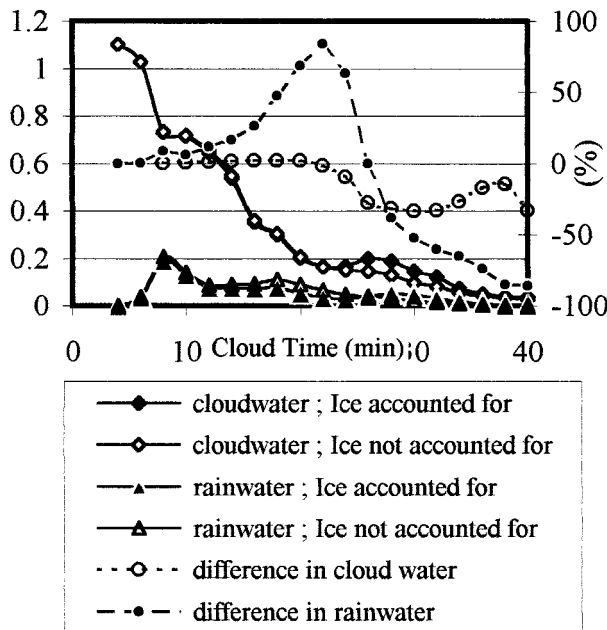


FIG. 9. Same as for Fig. 8 but for H_2O_2 in liquid phases.

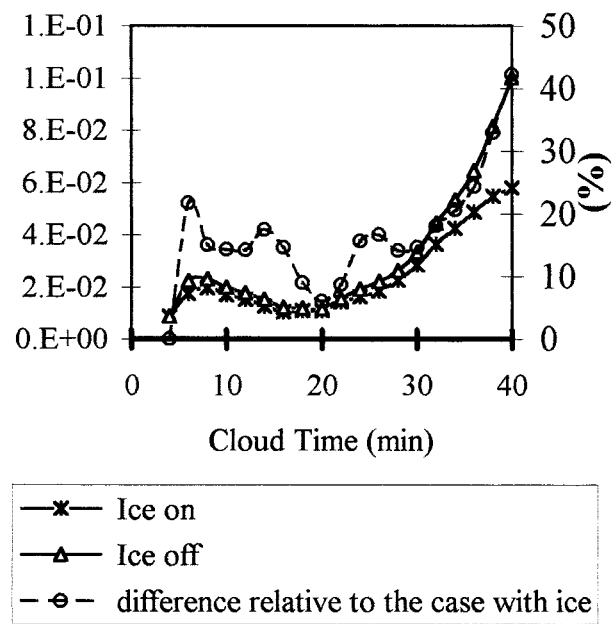


FIG. 11. Same as for Fig. 8 but for S(IV).

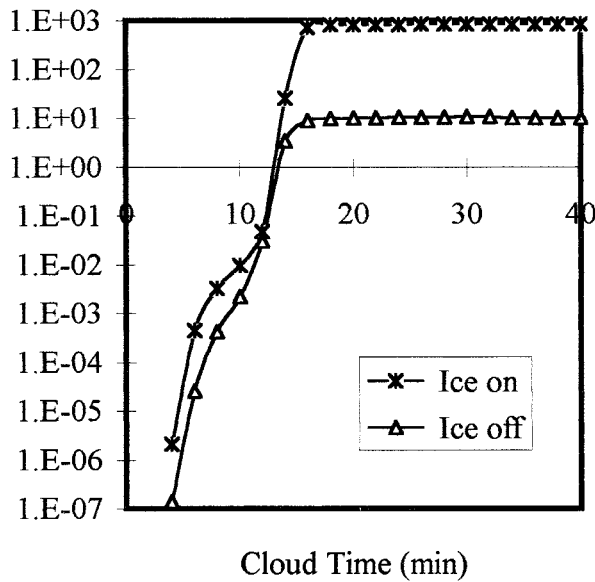


FIG. 12. Sulfates in gas phase averaged over the entire domain in the case with no initial sulfates aerosols.

enged by rain when ice is not accounted for in chemistry, are captured by graupel. Figure 17 points out that the total enhancement of condensed phase in sulfate content due to the presence of initial aerosols in the atmosphere is about 50%–60% for the mature and decaying stages of the cloud. However, the enrichment is higher in the development stage of the cloud, meaning that during the second and last stages of the cloud the losses by washout and release to the atmosphere by evaporation and riming of graupel efficiently counteract this uptake of aerosols.

Figure 19 illustrates how ice modifies the scavenging of aerosols. During the growth stage of the cloud no difference is seen over all condensed phases while nevertheless rainwater has a lower content in sulfates. This

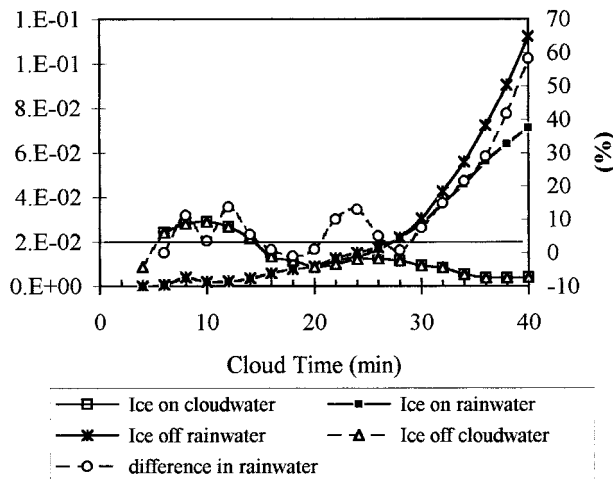


FIG. 13. Same as for Fig. 9 but for S(IV).

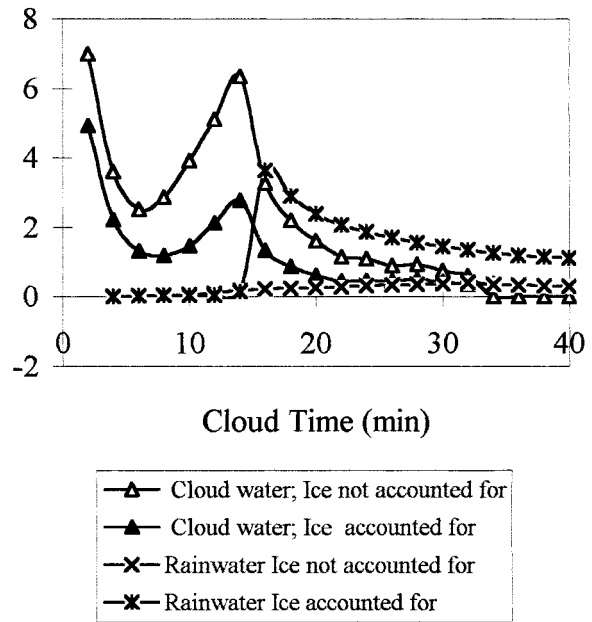


FIG. 14. Sulfates in liquid phases (averaged over the all cloud), in equivalent $\mu\text{g g}^{-1}$ water (no aerosols).

is again an effect of freezing droplets: sulfate aerosols are simply transferred to graupel. When riming becomes predominant, the sulfate content in rainwater is strongly enhanced (by a factor of 2). Over all condensed phases, the enrichment is lower (67%) due to the release in gas phase.

7. Conclusions

The sensitivity of chemistry to the ice phase has herein been studied in the framework of a cold-precipitating

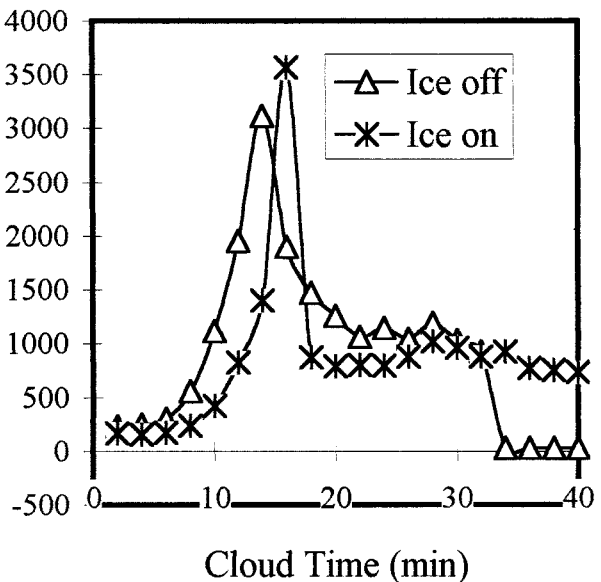


FIG. 15. As for Fig. 14 but in condensed phases.

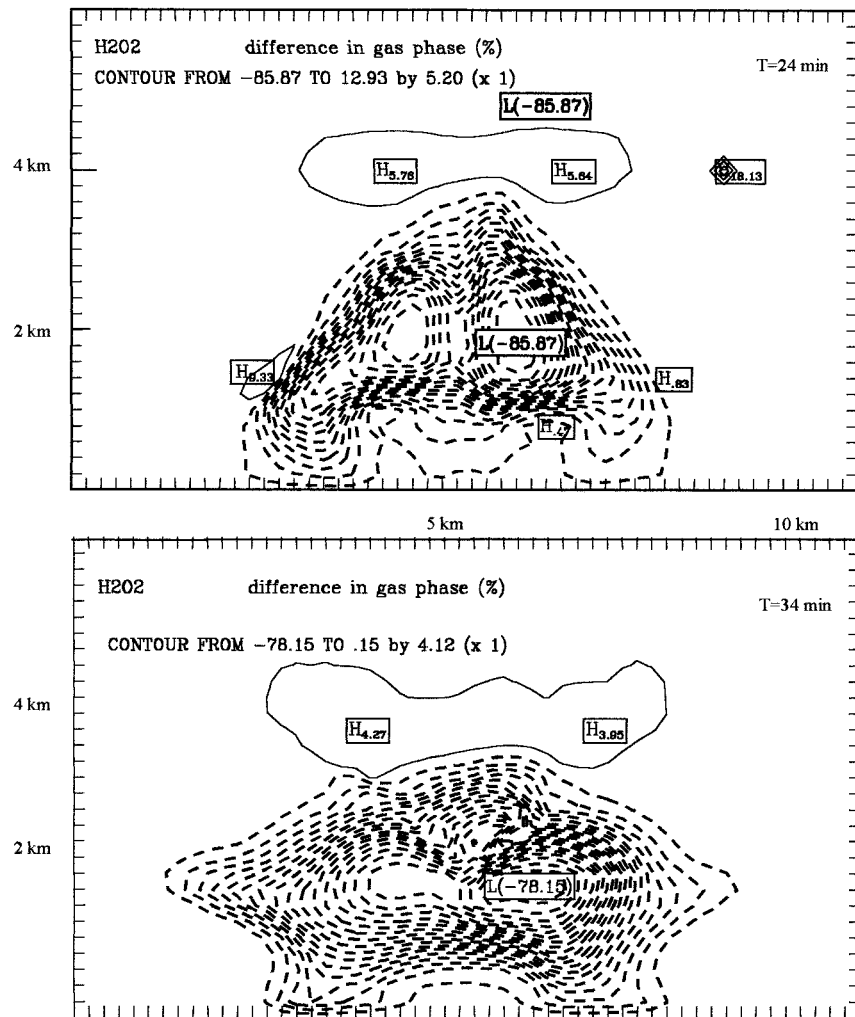


FIG. 16. Difference in gas phase concentrations of hydrogen peroxide expressed relatively to the case where ice is accounted for in the chemistry module (given in percent).

storm. The partitioning of the species between the different phases depends strongly on how many processes are dominant and which they are. The nature of these processes and their number (one or more process to be dominant) evolves following the stage of development of the cloud and can differ from one species to another. The reason for this last point comes from the fact that each species has its own solubility and retention coefficient. The scenario developed by this cumulonimbus cloud allows us to distinguish the following features.

- First, when freezing of drops and graupel riming are the dominant processes for the transfer of species from liquid phases to graupel, a change in sulfate production is observed. This change is made through a feedback effect of the riming process, that is, enhancement of the oxidation of SO_2 in sulfates in cloud droplets, reducing both SO_2 and H_2O_2 available for transfer to rain.
- Second, when only one process dominates the ex-

change of species with graupel, the result depends on whether it is the riming of graupel or freezing of drops. When riming is the main process both for SO_2 and H_2O_2 , the production of sulfate in rainwater is more efficient, whereas when freezing of drops is dominant for S(IV) a reduction of sulfate production in rain is observed.

- Finally, the decaying stage of the cloud allows a competition between riming and sedimentation processes. S(IV) is more sensitive than hydrogen peroxide to sedimentation effects, which induces a net decrease in its content in rainwater (subsequently over all condensed phases).

The chemical role of ice can be summarized as follows: there is an enrichment in precipitation in the oxidant H_2O_2 , while slightly more sulfates and less S(IV) are found in this precipitation (solid and liquid). Ice-phase processes also induce higher contents of sulfates in the gas phase as a consequence of the riming process.

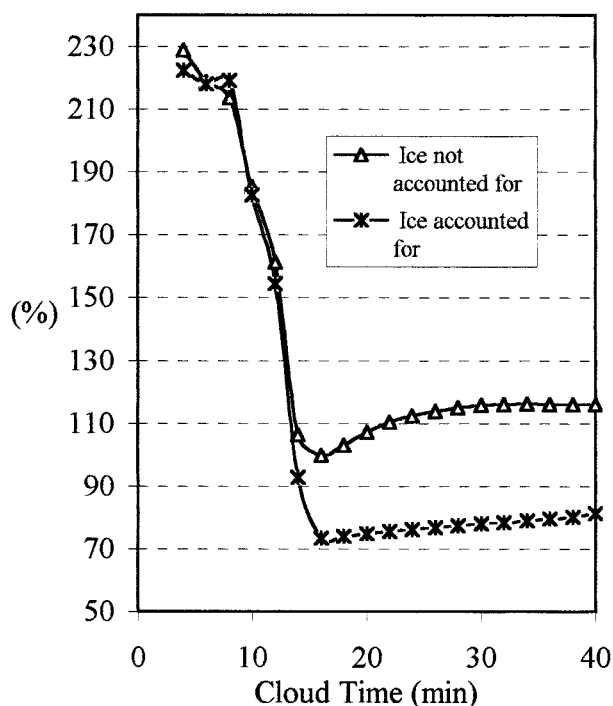


FIG. 17. Difference of sulfate concentrations in rainwater between runs with and without aerosols (expressed in percent relative to the case without aerosols).

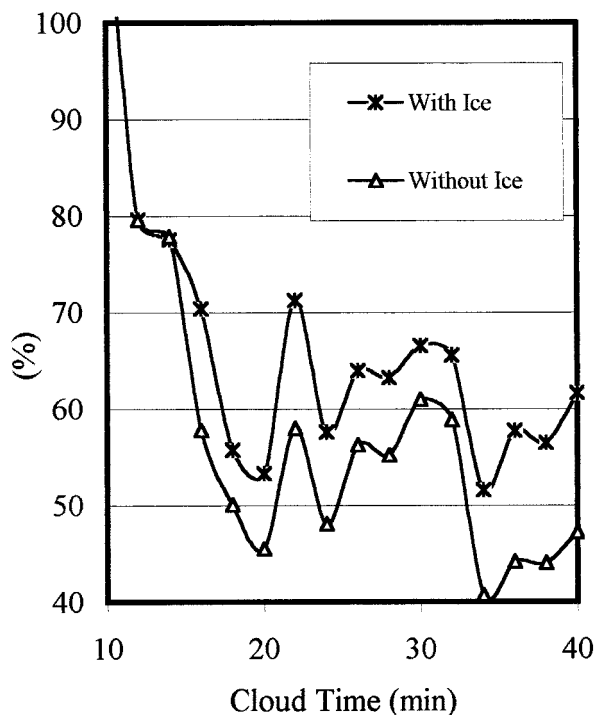


FIG. 18. Same as for Fig. 17 but for all condensed phases.

It is noteworthy that ice-phase microphysical processes do not act for aerosols as they do for gaseous species. For instance, when both riming and freezing play an equivalent role in the transfer of species to graupel, there is no feedback of riming on sulfate aerosols, as is the case for chemical species. A simple transfer of aerosols from rainwater to graupel is accomplished. When riming exists alone or in competition with sedimentation effects, the uptake of aerosols by rain is important. On the basis of a same mass of water, raindrops are more efficient than ice crystals given the fact that the maximum of rain mixing ratio only reaches 0.2 g kg^{-1} while the maximum value for graupel is 0.7 g kg^{-1} . Nevertheless, the fact that graupel covers a greater extent in this cloud means that its effect on chemistry and wash out of graupel must be accounted for in models.

This work shows how strongly nonlinear is the dependency of chemistry on ice-phase microphysical processes and that these latter interact together in a manner that can be specific to a species. Hence, for a given microphysical process, no overall effect on chemistry can be derived or generalized. They remain strongly interdependent. However, from one cloud to another, freezing of drops and riming will remain the dominant processes, and their effect on sulfate production, according to which of them is dominant, will probably be similar to the case studied here. Such complex interactions can explain why in winter storms the ratios of species in rainwater to that in cloud water are poorly

correlated to the rimed mass fraction (Mitchell and Borys 1992).

Finally, interactions with dynamics seem to be important in particular to disseminate effects obtained at a higher level. More detailed work should be done to study the sensitivity of the results obtained for sulfates

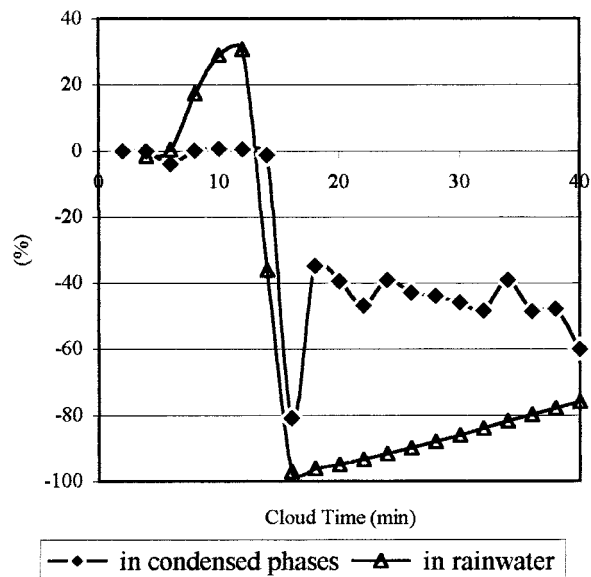


FIG. 19. Differences of sulfates contents due to the action of ice on chemistry in the case with initial aerosols in condensed phases and in rainwater, respectively.

to the retention coefficient for S(VI) [taken here as those of S(IV)]. A 3D framework will allow one to account for the storm displacement and the entrainment of fresh air into the cloud cell.

Acknowledgments. The work reported in this paper was supported by the INSU/CNRS (Institut National des Sciences de l'Univers/Centre National de la Recherche Scientifique) Program PNCA (Programme National de Chimie Atmosphérique). Computer resources were provided by I.D.R.I.S. (Institut du Développement et des Ressources en Informatique Scientifique), Project 187.

REFERENCES

- Barth, M. C., D. A. Hegg, and P. V. Hobbs, 1992: Numerical modeling of cloud and precipitation chemistry associated with two rainbands and some comparisons with observations. *J. Geophys. Res.*, **97**, 5825–5845.
- Cautenet, S., and B. Lefevre, 1994: Contrasting behavior of gas and aerosol scavenging in convective rain: A numerical and an experimental study in the African equatorial forest. *J. Geophys. Res.*, **99**, 13 013–13 024.
- Chameides, W. L., 1984: The photochemistry of a remote marine stratiform cloud. *J. Geophys. Res.*, **89**, 4739–4755.
- Chaumerliac, N., E. Richard, R. Rosset, and E. C. Nickerson, 1991: Impact of two microphysical schemes upon gas scavenging and deposition in a mesoscale meteorological model. *J. Appl. Meteor.*, **30**, 88–97.
- Cotton, W. R., M. A. Stephens, T. Nehr Korn, and G. J. Tripoli, 1982: The Colorado State University 3-dimensional cloud mesoscale model. Part II: An ice phase parameterization. *J. Rech. Atmos.*, **16**, 295–320.
- Daum, P. H., S. E. Schwartz, and L. Newman, 1984: Acidic and related constituents in liquid water stratiform clouds. *J. Geophys. Res.*, **89**, 1447–1460.
- DeMore, W. B., and Coauthors, 1994: Chemical kinetics and photochemical data for use in stratospheric modeling. Evaluation No. 11, California Institute of Technology, Pasadena, CA. [Available from California Institute of Technology, 1200 East California Blvd, Pasadena, CA 91125.]
- Diehl, K., S. K. Mitra, and H. R. Pruppacher, 1998: A laboratory study on the uptake of HCl, HNO₃, and SO₂ gas by ice crystals and the effect of these gases on the evaporation rate of the crystals. *Atmos. Res.*, **47–48**, 235–244.
- Hegg, D. A., S. A. Rutledge, and P. V. Hobbs, 1984: A numerical model for sulfur chemistry in warm-frontal rainbands. *J. Geophys. Res.*, **89**, 7133–7147.
- , —, and —, 1986: A numerical model for sulfur and nitrogen scavenging in narrow cold-frontal rainbands. 2. Discussion of chemical fields. *J. Geophys. Res.*, **91**, 14 403–14 416.
- Iribarne, J. V., and L. A. Barrie, 1995: The oxidation of S(IV) during riming by cloud droplets. *J. Atmos. Chem.*, **21**, 97–114.
- Kelly, T. J., P. H. Daum, and S. E. Schwartz, 1985: Measurement of peroxides in cloudwater and rain. *J. Geophys. Res.*, **90**, 7861–7872.
- Kessler, E., 1969: *On the Distribution and Continuity of the Water Substance in Atmospheric Circulation*. Meteor. Monogr., No. 32, Amer. Meteor. Soc., 84 pp.
- Lamb, D., and R. Blumenstein, 1987: Measurements of the entrainment of sulfur dioxide by rime ice. *Atmos. Environ.*, **21**, 1765–1772.
- Leighton, H. G., M. K. Yau, A. M. McDonald, J. S. Pitre, and A. Giles, 1990: A numerical study of the chemistry of a rainband. *Atmos. Environ.*, **24A**, 1211–1217.
- Lelieveld, J., and P. J. Crutzen, 1991: The role of clouds in tropospheric photochemistry. *J. Atmos. Chem.*, **12**, 229–267.
- Marshall, J. S., and W. M. Palmer, 1948: The distribution of raindrops with size. *J. Meteor.*, **5**, 165–166.
- Mitchell, D. L., and R. D. Borys, 1992: A field instrument for examining in-cloud scavenging mechanism by snow. *Precipitation Scavenging and Atmosphere-Surface Exchange*, S. Schwartz and W. G. N. Slinn, Eds., 239–255.
- Mitra, S. K., S. Barth, and H. R. Pruppacher, 1990: A laboratory study on the scavenging of SO₂ by snow crystals. *Atmos. Environ.*, **24A**, 2307–2312.
- Mölder, N., H. Hass, H. J. Jakobs, M. Laube, and A. Ebel, 1994: Some effects of different cloud parameterizations in a mesoscale model and a chemistry transport model. *J. Appl. Meteor.*, **33**, 527–545.
- Murakami, M., T. Kimura, C. Magono, and K. Kikuchi, 1983: Observations of precipitation scavenging for water soluble particles. *J. Meteor. Soc. Japan*, **61**, 346–358.
- Oberholzer, B., M. Volken, J. R. Collet, J. Staehelin, and A. Waldvogel, 1993: Pollutant concentrations and below-cloud scavenging of selected N-(III) species along a mountain slope. *Water, Air, Soil Pollut.*, **68**, 59–73.
- Orville, H. D., and F. J. Kopp, 1977: Numerical simulation of the life history of a hailstorm. *J. Atmos. Sci.*, **34**, 1596–1618.
- Reisin, T., Z. Levin, and S. Tzivion, 1996: Rain production in convective clouds as simulated in an axisymmetric model with detailed microphysics. Part I: Description of the model. *J. Atmos. Sci.*, **53**, 497–519.
- Respondek, P. S., A. I. Flossmann, R. R. Alheit, and H. R. Pruppacher, 1995: A theoretical study of the wet removal of atmospheric pollutants. Part V: The uptake redistribution and deposition of (NH₄)₂SO₄ by a convective cloud containing ice. *J. Atmos. Sci.*, **52**, 2121–2132.
- Rutledge, S. A., D. A. Hegg, and P. V. Hobbs, 1986: A numerical model for sulfur and nitrogen scavenging in narrow cold-frontal rainbands. 1. Model description and discussion of microphysical fields. *J. Geophys. Res.*, **91**, 14 403–14 416.
- Sigg, A., T. Staffelbach, and A. Neftel, 1992: Gas phase measurements of hydrogen peroxide in Greenland and their meaning for the interpretation of H₂O₂ records in ice cores. *J. Atmos. Chem.*, **14**, 223–232.
- Snider, J. R., D. C. Montague, and G. Vali, 1992: Hydrogen peroxide retention in rime ice. *J. Geophys. Res.*, **97**, 7569–7578.
- Song, O., and H. Leighton, 1996: Parameterization of in-cloud sulfate production. *Extended Abstracts, WMO Conf. on Cloud Physics*, Zurich, Switzerland, 1216–1219.
- Stockwell, W. R., 1994: Effects of gas-phase chemistry on aqueous-phase sulfur dioxide rates. *J. Atmos. Chem.*, **19** (3), 317–325.
- Taylor, G. R., 1989a: Sulfate production and deposition in midlatitude continental cumulus clouds. Part I: Cloud model formulation and base run analysis. *J. Atmos. Sci.*, **46**, 1971–1990.
- , 1989b: Sulfate production and deposition in midlatitude continental cumulus clouds. Part II: Chemistry model formulation and sensitivity analysis. *J. Atmos. Sci.*, **46**, 1991–2006.
- Topol, L. E., 1986: Differences in unique compositions and behaviour in winter rain and snow. *Atmos. Environ.*, **20**, 347–355.
- Tremblay, A., and H. Leighton, 1986: A three-dimensional cloud chemistry model. *J. Climate Appl. Meteor.*, **25**, 652–671.
- Wang, C., and J. S. Chang, 1993: A three-dimensional numerical model of cloud dynamics, microphysics and chemistry. I. Concept and formulation. *J. Geophys. Res.*, **98**, 14 827–14 844.
- Zhang, D. L., 1989: The effect of parameterized ice microphysics on the simulation of vortex circulation with a mesoscale hydrostatic model. *Tellus*, **41A**, 132–147.